Hemodynamics of gastric microcirculation in rats

JÁNOS PETI-PETERDI, GERGELY KOVÁCS, PÉTER HAMAR, AND LÁSZLÓ ROSIVALL
Institute of Pathophysiology, Semmelweis University Medical School, Budapest H-1089, Hungary

Peti-Peterdi, János, Gergely Kovács, Péter Hamar, and László Rosivall. Hemodynamics of gastric microcirculation in rats. *Am. J. Physiol.* 275 (*Heart Circ. Physiol.* 44): H1404–H1410, 1998.—Recently, we described a novel preparation of rat stomach for vascular micropuncture studies. The aim of the present study was to directly measure basic microvascular parameters along the length of the gastric vasculature. Blood vessels were identified, and intravascular pressure was measured with a servo-null transducer, vessel dimensions with videometry, blood flow with microspheres, and plasma colloid osmotic pressure with an osmometer. When systemic arterial pressure was 100–110 mmHg, intravascular pressures in small arteries, primary, secondary, and tertiary submucosal arterioles, mucosal terminal arterioles, and muscle arterioles were 77.8 ± 2.6, 74.6 ± 2.5, 54.1 ± 1.8, 34.4 ± 1.6, 32.4 ± 1.2, and 30.5 ± 1.4 (SE) mmHg, respectively. Intravascular pressures in collecting veins, secondary and primary submucosal venules, muscle venules, and small veins were 26.6 ± 1.1, 21.8 ± 1.6, 17.1 ± 0.8, 18.2 ± 0.9, and 14.4 ± 0.6 mmHg, respectively. Capillary pressure in the mucosa (28 mmHg), as estimated by interpolation between terminal arteriole and collecting venule pressures, was significantly higher than in the muscle layer (23.6 ± 1.4 mmHg). A total of 155 vessels from 25 animals were sampled. Relative blood flows were 16 ± 3% in the muscle and 84 ± 3% in the mucosa-submucosa. Analysis of filtration forces in these two different capillary beds suggests that gastric mucosal capillaries are primarily a filtering network, whereas muscle capillaries are in fluid balance. Calculated resistance ratios indicate low precapillary but relatively high postcapillary vascular resistance in the gastric mucosa.

microvascular pressures; gastric vasculature; blood flow distribution; vascular resistance; transcapillary fluid exchange

INTRAVASCULAR PRESSURES have been measured using micropuncture techniques in several organs, including the small intestine (13); however, direct information on the gastric circulation is lacking. Capillary hydrostatic pressures and other basic microcirculatory factors governing transcapillary fluid exchange in the stomach have been calculated indirectly or estimated from other measured parameters of the Starling equation (15, 16). These estimations, however, were speculative and based on data obtained with inherently limited methods. Recently, we developed an in vivo micropuncture method to measure intravascular pressures of various microvessels in the muscle and submucosal and mucosal layers of the gastric wall (29). This technique provides a means to obtain direct measurements of gastric microvascular parameters.

Previous studies have found significant regional differences in capillary pressure and net transcapillary fluid movement between the three major regions of the small intestine (13, 14), i.e., mesentery, intestinal muscle, and mucosal layers. This finding implies that microvascular regions in the gastrointestinal tract may continuously filter (mesentery) or absorb (mucosa), whereas those in other regions (muscle) may be in fluid balance. Because the stomach is a secretory organ, further variations in capillary pressures could be found. Furthermore, it has been well accepted that the intact mucosal microcirculation is an essential factor in the ability of the gastric mucosa to maintain its integrity against various aggressive factors (19, 31, 37). Therefore, exact knowledge of gastric microcirculatory and transcapillary fluid exchange parameters may also have importance in understanding the mechanisms of mucosal protection.

The purpose of this study was to determine the profile of intravascular pressures along the length of the gastric vasculature. The intramural blood flow distribution between gastric muscle and submucosal-mucosal layers was also measured so that precapillary-to-postcapillary resistance ratios could be calculated. Net transcapillary fluid movement across the muscle and mucosal microcirculation was also estimated, thereby providing an overall estimate of the Starling forces that occur within various regions of the stomach.

METHODS

The methods used to prepare the submucosal and deep mucosal layers of the gastric muscle for micropuncture studies are described briefly below. Details of this technique have been described in a recent report (29).

Animal Preparation

Male Wistar rats, weighing ~200 g, were fasted overnight with free access to water. Rats were anesthetized with thiobutabarbital sodium (Inactin-BYK, 120 mg/kg body wt ip) and placed on a micropuncture table, and body temperature was maintained at 37 ± 0.5°C by means of a heating pad controlled by a rectal thermistor probe. A tracheotomy was performed, and the trachea was intubated to facilitate spontaneous breathing. Systemic arterial blood pressure was monitored continuously through a PE-50 catheter placed in the left femoral artery and connected to a Statham electromanometer (model P23). A long, heparinized catheter (PE-50) was inserted into the left femoral vein, and Ringer solution (1.5 $ml \cdot h^{-1} \cdot 100$ g body wt^{-1}) was infused throughout the surgical preparation and experimental periods; this preparation was also used to measure systemic venous pressure.

Tissue Preparation

The abdomen was opened via a 5-cm midline incision, the stomach was gently exteriorized, and surrounding gastric

The costs of publication of this article were defrayed in part by the payment of page charges. The article must therefore be hereby marked "*advertisement*" in accordance with 18 U.S.C. Section 1734 solely to indicate this fact.

ligaments were cut. The exposed stomach was continuously bathed in warmed Ringer solution to avoid desiccation and irreversible cessation of blood flow in the superficial blood vessels. The animal was positioned on its right side on the micropuncture table, and the stomach was placed in a gastric chamber. The heating pad and continuous superfusion (1 ml/min) of warm Ringer solution kept the vascularly intact and innervated stomach in a constant environment with high humidity and a temperature of 37 ± 1°C. To stabilize the preparation with the posterior wall facing up, four small pins were inserted into the chamber wall through the esophagus, antrum, forestomach, and corpus (see diagram of gastric chamber and instrument setup in Ref. 29). However, to avoid respiration-induced gastric movements and changes in macrovascular parameters (e.g., venous pressure elevation) due to stretch, the esophagus was not tightly fixed. Care was taken to prevent compression or excessive manipulation of the left gastric artery, vein, and nerves to the stomach.

Vessels in different layers of the gastric wall were approached from the serosal side. A very light rubber ring was mounted over the gastric surface to serve as a reservoir for a film of fluid that was needed for the micropuncture technique (see diagram of gastric chamber and instrument setup in Ref. 29). The narrow gap between the rubber ring and the preparation was sealed with agar gel. The area inside the ring functioned as a working window, where the tip of the superfusion system was located. The working window consisted of two parts, the seromuscular and submucosal areas, each supplied by different small arteries. The seromuscular area served for micropuncture measurements in vessels of the muscle layer. To approach the submucosal and deep mucosal vasculature, a 1-cm-diameter piece of seromuscular tissue on the posterior wall of the corpus was removed by careful dissection from an area free of large vessels. In a small area of this submucosal preparation, we totally removed the submucosal connective tissue and the superficial part of the muscularis mucosae. In this way, the microvessels in the basal mucosa also became accessible through the remaining thin muscularis mucosae. After completion of the experimental setup, the tissue was allowed to equilibrate for 1 h before any experiments were attempted. Vascular reactivity was well preserved, and the minimal exteriorization procedure did not have significant adverse effects on the vessels under study, as have been assessed and tested in our recent report (29).

Measuring Techniques

The preparation, illuminated with an fiber-optic illuminator (Intralux 4000-1, Volpi), was visualized using a zoom stereomicroscope (model M8, Wild). Pressures were measured in microvessels with a servo-null transducer (model 4A, IPM) (20, 21, 36). A Leitz micromanipulator was used to insert sharpened micropipettes (0.5–2 μm) into selected vessels. Each micropipette was calibrated over the range 0–200 mmHg in a calibration chamber using a manometer. Microvascular pressure and systemic arterial blood pressure were recorded simultaneously on a recorder (model OH-814/1, Radelkis). Microvessel images were viewed through the microscope with a television camera (model SSC-M370CE, Sony), continuously displayed on a television monitor (model PVM-145E, Sony), and recorded on a videocassette recorder (model SLV815VP, Sony). Vessel dimensions were determined using the microscope eyepiece micrometer and measured in video recordings displayed on the television screen with a caliper.

In a separate series of experiments, we studied intramural blood flow distribution between gastric muscle and submucosal-mucosal layers using the Dye-Trak microsphere technique (3, 24). All reagents and disposable supplies were obtained from Fisher Scientific. Approximately 10^6 red microspheres, 15 μm diameter (Triton Technology, San Diego, CA) and suspended in 1 ml of saline containing 0.05% Tween 80, were injected into the ascending aorta over a 10-s period through a catheter placed into the right carotid artery. At 5 s before microsphere injection, a 30-s microsphere reference sample was collected by free-flow technique into a heparin-coated glass tube from the distal abdominal aorta through a cannula inserted into the left femoral artery. Two minutes after injection, the rat was killed, and the stomach was removed and divided into muscle and submucosal-mucosal layers by manual dissection. Each tissue and reference blood sample was weighed and then digested in glass tubes with 7 ml of 4 M KOH. The volume of the reference blood sample was calculated by weight according to the specific gravity (30). The digested tissue solution was filtered through a polyester filter with a pore size of 10 μm (Triton Technology) in a glass microanalysis filter holder (model 09-735G, Fisher Scientific). After filtration, microspheres were quantified by their dye content recovered by addition of 300 μl of dimethylformamide. The photometric absorption of each dye solution was determined using a spectrophotometer (model 8452A, Hewlett-Packard), and blood flow to each layer was calculated from the following relationship

$$\dot{Q}_B = 100\ (AU_L\ WR)/(AU_R\ LW)$$

where $\dot{Q}_B$ is blood flow ($ml \cdot min^{-1} \cdot 100\ g^{-1}$), AU_L is absorbance unit per layer sample, WR is reference blood flow rate (ml/min), AU_R is absorbance unit per reference blood sample, and LW is layer weight (g). The relative blood flow of gastric muscle or submucosal-mucosal layers was calculated as follows

$$R = 100\ (AU_L)/(AU_{mus} + AU_{muc})$$

where R is the percent ratio of total gastric blood flow and AU_{mus} and AU_{muc} are the absorbance units of muscle and submucosal-mucosal layer samples, respectively.

Plasma colloid osmotic pressure was measured from plasma samples using a colloid osmometer as described by Aukland and Johnsen (4).

Data were analyzed with a statistical software package (SigmaStat for Windows, Jandel Scientific). ANOVA was applied for intergroup comparison of intravascular pressure data from different vessel types. Values are means ± SE. $P < 0.05$ was considered significant.

RESULTS

Vessel Identification and Description of Vascular Architecture

Microvessels in rat gastric wall were identified (Fig. 1) according to branching hierarchy and relative dimensions or with a descriptive classification similar to the system proposed by Wiedeman (35) and applied to the small intestine by Gore and Bohlen (13).

The posterior branch of the left gastric artery, a major branch of the celiac axis, gives rise to a series of long vessels supplying the posterior corpus. These vessels pierce the external muscle layers at the lesser curvature near the cardia and run under the muscle coat in the superficial submucosa radially toward the greater curvature. The diameter of these small arteries (SA) is 89.1 ± 2.1 μm.

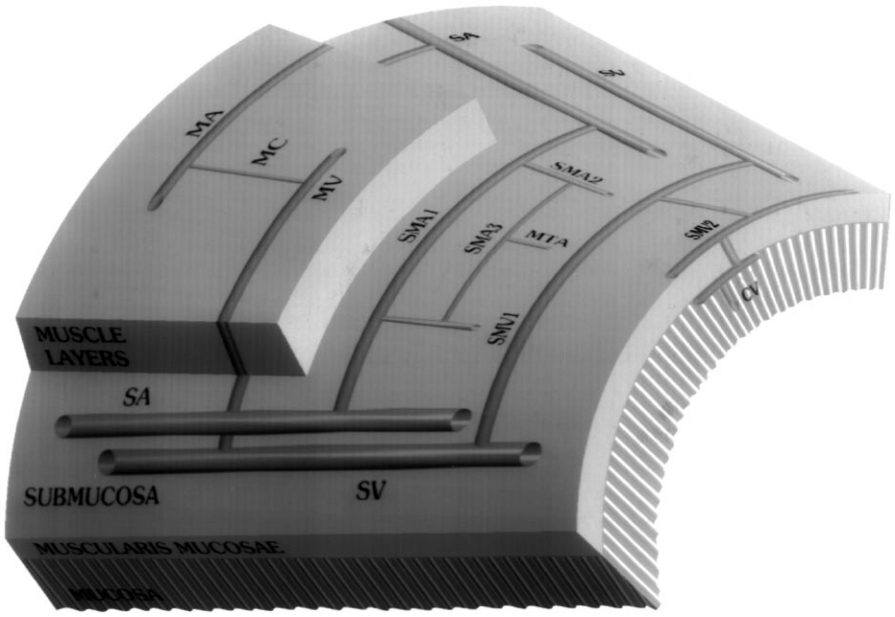

Fig. 1. Schematic representation of microvasculature in gastric wall. Blood vessels were identified numerically according to their branching order and vascular hierarchy: small artery (SA), submucosal primary (SMA1), secondary (SMA2), and tertiary (SMA3) arterioles, mucosal terminal arteriole (MTA), collecting venule (CV), submucosal secondary (SMV2) and primary (SMV1) venules, muscle arteriole (MA), capillary (MC), and venule (MV), and submucosal small vein (SV). Common input and output of muscle and mucosal circulations are SMA1 and SMV1.

Submucosal and deeper mucosal vasculature. Through the process of anastomoses, small arteries form the main submucosal arterioarterial anastomotic plexus or primary arcade of submucosal arterioles (SMA1) and average 75.5 ± 1.8 μm in diameter. In turn, these vessels form smaller and smaller branches, which interconnect with each other and the parent vessels forming a secondary and a tertiary arcade of submucosal arterioles (SMA2 and SMA3, 42.3 ± 1.6 and 24.4 ± 0.8 μm, respectively). These arcades form a very extensive, interconnecting arterial network in the submucosa. The tertiary arcade gives rise to small mucosal terminal arterioles (MTA, 15.5 ± 0.7 μm), which run perpendicularly through the muscularis mucosae and, on entering the mucosa, divide into the hexagonal mucosal capillary plexus. Collecting veins (CV) run perpendicularly through the mucosa and, on cross section, appear as dark round dots that are 36.4 ± 1.1 μm diameter. Within the deeper mucosa they drain into the venous anastomosis, which, on entering the muscularis mucosae, gives rise to the secondary arcade of submucosal venules (SMV2). This observation of the mucosal venous architecture is somewhat different from previous descriptions (12, 17, 32); however, the existence of a deep mucosal venous anastomosis is further supported by a recent study (27). Interestingly, collecting venules were larger in diameter (36.4 ± 1.1 μm) than the deeper mucosal venous anastomosis (31.5 ± 1.3 μm) or the initial part of SMV2. SMV2 are larger than their respective arteries (55.8 ± 1.3 μm) and interconnected in a similar manner. SMV2 enter the primary arcade of submucosal venules (SMV1, 87.5 ± 1.6 μm), which follow the same course as the primary arterioles and return blood to the small veins (SV, 99.1 ± 1.8 μm). These SV run parallel with SA, penetrate the external muscle layers, and leave the superficial submucosa.

Muscle vasculature. SA or initial parts of SMA1 give rise to ascending muscle arterioles, which supply muscle arterioles (MA, 16.6 ± 0.8 μm diameter) in the circular and longitudinal muscle layers. These arterioles run perpendicularly to the muscle fibers and divide into the longitudinal and circular muscle capillaries (MC, 4.8 ± 0.4 μm), which run parallel to the muscle fibers. Capillaries end in muscle venules (MV, 23.2 ± 0.9 μm), which form descending venules through both muscle layers and return blood to the SMV1 or SV before leaving the submucosa. Figure 2 shows an ink-stained preparation of gastric vasculature and the various branches of the gastric circulation.

Intravascular Pressure Distribution

Microvascular pressure was measured for up to 5 h with no signs of deterioration of the tissue as judged by the absence of leukocytes sticking and rolling along the walls of venules or progressive dilatation of arterioles and large-amplitude vasomotion. In most animals, spontaneous gastric muscle contractions and respiratory movements were small enough to allow micropuncture measurements. The results of microvascular pressure and dimension measurements are summarized in Figure 3. A total of 155 vessels from 25 animals were sampled. Systemic arterial and venous blood pressure averaged 108 ± 2 and 7 ± 0.5 mmHg, respectively.

Submucosal and deeper mucosal vasculature. Pressures in submucosal SA averaged 77.8 ± 2.6 mmHg. Only slightly lower pressures were measured in SMA1 (74.6 ± 2.5 mmHg), which is not surprising, since SMA1 are shunt vessels between adjacent small arteries. About one-half of the systemic pressure was found in SMA2 (54.1 ± 1.8 mmHg). Pressures in SMA3 averaged 34.4 ± 1.6 mmHg, significantly less than in SMA2 but similar to the pressures in MTA (32.4 ± 1.2 mmHg). Pressures in CV, SMV2, SMV1, and SV were 26.6 ± 1.1, 21.8 ± 1.6, 17.1 ± 0.8, and 14.4 ± 0.6 mmHg, respectively. Mucosal capillary pressure was estimated from input (MTA) and output (CV) pressures

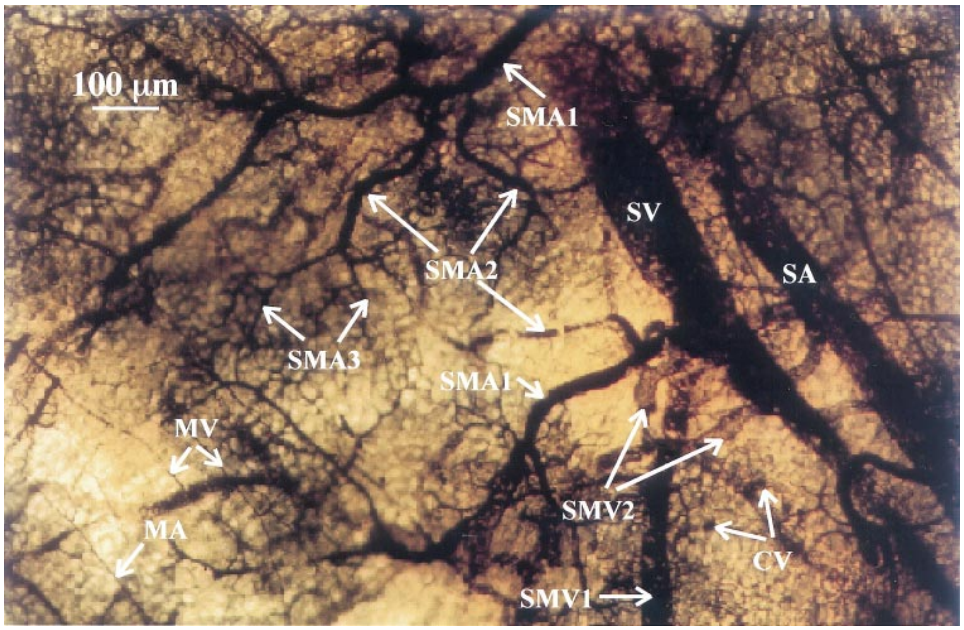

Fig. 2. Micrograph of gastric microvasculature injected with india ink. See Fig. 1 legend for vessel identification.

of the mucosal capillary network by calculating the mean and resulted in 28 mmHg. The validity of this estimation was tested using intravascular pressure data obtained from the muscle microvasculature. Because the difference between calculated (24.3 mmHg) and measured (23.6 ± 1.4 mmHg) MC pressure was not significant, the value of 28 mmHg for mucosal capillary pressure was accepted.

Muscle vasculature. Pressures were not measured in ascending arterioles or descending venules because of technical difficulties. However, the greatest pressure drop was apparent across these arterioles, since the MA pressure was 30.5 ± 1.4 mmHg, less than one-half of SMA1 pressure. Microvascular pressure further decreased to 23.6 ± 1.4 mmHg in the MC and to 18.2 ± 0.9 mmHg in MV. Figure 4 compares precapillary, capillary, and postcapillary hydrostatic pressures from muscle and mucosal layers.

Intramural Blood Flow Distribution

Absolute and relative blood flows to gastric muscle and mucosal layers were measured in 11 additional animals. Because the submucosal and mucosal microvasculatures are coupled and cannot be separated by manual dissection, we report mucosal and submucosal flows as a single value. However, the scarcity of submucosal capillaries would suggest that submucosal flow is only a small fraction of total gastric blood flow. Absolute flows to the muscle and submucosal-mucosal regions averaged 70.4 ± 22.3 and 120.8 ± 18.8 ml·min^{-1}·100 g^{-1}, respectively. From calculation of the relative blood flow distribution, the gastric muscle layer received 16 ± 3% and the submucosa-mucosa 84 ± 3% of total gastric blood flow. These results are comparable to those from other studies (3, 5, 11).

Plasma colloid osmotic pressure was measured from 27 samples of 25 animals; it averaged 18.9 ± 1.7 mmHg and is within the normal range (38).

DISCUSSION

Microvascular pressures have been measured in different organs, including the small intestine (13), but studies from gastric microvessels are lacking. Previously, gastric mucosal hydrostatic capillary pressure has been estimated from the balance of Starling forces, resulting in a value of 10.6 mmHg (15, 16). In contrast, we found that mean capillary pressure in different regions of the gastric vasculature ranges from 20 to 30 mmHg, values that are significantly higher than previously calculated. This discrepancy may be explained

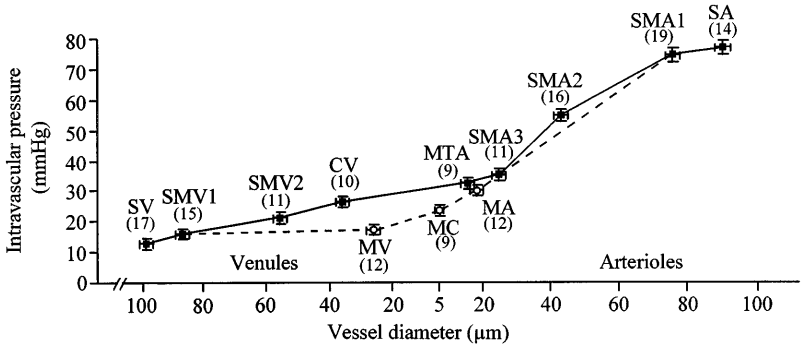

Fig. 3. Intravascular pressure distribution in gastric vasculature. Data were recorded from muscle (○) and mucosal blood vessels (■) at systemic arterial pressures of 100–110 mmHg. See Fig. 1 legend for vessel identification. Values are means ± SE; *n*, number of vessels. A total of 155 vessels from 25 animals were sampled.

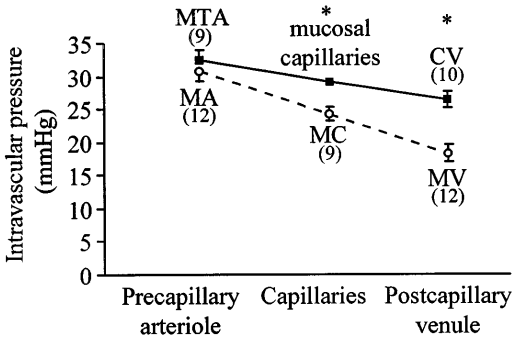

Fig. 4. Precapillary, capillary, and postcapillary hydrostatic pressures in muscle (○) and mucosal regions (■) of gastric vasculature. See Fig. 1 legend for vessel identification. Values are means ± SE; *n*, number of vessels. *$P < 0.05$ compared with corresponding segment in muscular circulation (by ANOVA).

partly by inherent limitations in the methods used in previous calculations. For example, the rate of lymph flow was used as an estimate of net capillary filtration rate (6). However, lymph flow may not accurately reflect capillary filtration rate if significant transepithelial fluid secretion or absorption occurred during the period in which lymph flow was measured. In secreting organs, such as the stomach, capillary filtration rate could be significantly underestimated by lymph flow, since a proportion of the capillary filtrate would be removed from the interstitial spaces via the transporting epithelia rather than the lymphatics. Furthermore, previous calculations of Starling forces used a value of interstitial fluid pressure measured with microcapsules implanted in the gastric submucosa (1). Because this layer of the gastric wall has only a few nutritive capillaries compared with the dense mucosal capillary system, tissue factors governing transcapillary fluid exchange in the submucosa are most probably different from those of the mucosa.

Another factor that could significantly modify microcirculatory hydrostatic pressures is muscle activity. Many studies have shown that the motor activity of the intestine can affect blood flow (8–11, 18, 23, 33). In these experiments a large increase in intramural pressure produced by distension or prolonged tonic contraction was accompanied by an increased local vascular resistance. Changes in blood flow have been explained as a result of passive changes in vessel caliber due to changes in vascular transmural pressure subsequent to alterations in motility. In our preparation, muscle contractions can also increase passive resistance of blood vessels. SA, SV, and ascending arterioles and descending venules run perpendicularly to the outer muscle layers. Furthermore, MTA and SMV2 penetrate the muscularis mucosae in a similar manner. Ample evidence has been presented (1) that the basal tone of gastric muscles and peristaltic waves also increase the interstitial fluid pressure. In comparison to earlier methods (7, 17, 32), in which gastric or intestinal wall and muscle were transected and the mucosa was exteriorized, in our preparation the whole stomach was fixed in the gastric chamber without surgery. Thus the effect of tonic muscle contraction on vascular and interstitial hydrostatic pressure was included in our experimental results. However, because of this lack of exposure, we could not measure mucosal interstitial fluid pressure by direct micropuncture. On the other hand, we could not document the possible effect of peristalsis on intravascular pressure (i.e., oscillation in pressure), because, as a result of contractions, small vessels could be penetrated for a relatively short period (15–20 s). Also, oxygen is a potent vasoconstrictor, and high oxygen superfusates (such as those equilibrated with room air) have long been known to cause arteriolar constriction and decreased blood flow in exteriorized tissues (22, 25, 34). Most intravital microscopy studies use a superfusate equilibrated with a 0 or 5% oxygen gas mixture to prevent abnormally high oxygen levels in the tissue. This ensures that tissue oxygenation is achieved solely by blood oxygen delivery (as it is in situ) and that the superfusate is not a source of additional oxygen. Therefore, our high-oxygen superfusate could have had some effect on arteriolar tone and the microvascular pressure profile, although we did not observe any indication of such vasoconstriction.

Digestive juices are secreted each day by the salivary glands, stomach, pancreas, liver, and small intestine. Although emphasis has been placed on the importance of the epithelium in secretory transport of fluid in digestive organs, the role of the microcirculation in transporting fluid to and from the epithelium has received relatively little attention. We found that mean capillary pressure in the gastric mucosa was 28 mmHg, whereas plasma oncotic pressure was 18.9 ± 1.7 mmHg. With the use of these values together with additional data from other studies, it is possible to estimate filtration forces in the gastric mucosal microcirculation. If we consider the values of gastric lymph protein concentration and osmotic reflection coefficient (28) and assume a small positive value for the interstitial fluid pressure (1), there is a 10- to 15-mmHg net driving force for transcapillary filtration. A total safety factor against edema formation (increased lymph flow, interstitial fluid pressure, transcapillary oncotic pressure gradient) has been described for intestinal mucosa and ranges from 12 to 15 mmHg (26). Thus, from this information, gastric mucosal interstitium may be well hydrated and close to fluid imbalance under resting conditions. These conditions may thereby supply the fluid necessary for active epithelial secretion. Further increments in mucosal capillary pressure in excess of 15 mmHg, which may happen during peristaltic muscle contractions, particularly those of the muscularis mucosae, may lead to enhanced passive gastric secretion. Evidence has been shown that increases in interstitial fluid pressure are associated with alkaline fluid secretion across the gastric mucosa (2). Flow of interstitial fluid across the gastric mucosa (so-called gastric filtration) has been observed under a variety of experimental conditions, e.g., elevation of arterial and venous pressure and intra-arterial infusion of ACh, which leads to increased capillary filtration and strong muscular activity (2). Thus one can further speculate that, during peristaltic muscle contractions, high mucosal capillary

pressure results in elevated interstitial hydrostatic pressure and an enhanced alkaline fluid secretion, and this may play an important role in protection against luminal acidity.

We found that capillary pressure in the gastric muscle layer was significantly less (23.6 ± 1.4 mmHg) than the calculated mean capillary pressure in the mucosa (28 mmHg) at normal systemic arterial pressures (100–110 mmHg; Fig. 4). This suggests that the Starling forces across the muscle microcirculation may be closer to equilibrium. This idea is further supported by the anatomic difference between the two capillary beds; i.e., mucosal capillaries are of the fenestrated type, whereas those in the muscularis are of the less permeable continuous type. Our findings are consistent with direct pressure measurements by Gore and Bohlen (13, 14) from the rat small intestine, which showed regional differences in capillary hydrostatic pressure between muscle and mucosal layers. They suggested that mesenteric capillaries are primarily a filtering network; intestinal muscle capillaries are normally in fluid balance, whereas, at rest, intestinal mucosal capillaries are primarily absorptive. These findings imply that there are regional differences in transcapillary fluid exchange in the gastrointestinal tract, whereas the whole organ is essentially in fluid balance.

The gastric vasculature is composed of two structurally different microvascular beds, which are connected in parallel at the level of the submucosa. Microsphere measurements indicated that, under resting conditions, the mucosa-submucosa receives 84 ± 3% of the total gastric blood flow and the muscularis 16 ± 3%. These findings are consistent with previous work using similar techniques (3, 5, 11). Differences in intravascular pressure distribution between the muscle and the mucosal region may be explained in terms of differences in vascular morphology, architecture, and relative resistances in the two regions. In Fig. 3 the arterial pressure drop down to the precapillary arterioles was almost identical; pressure was 32.4 ± 1.2 mmHg in MTA and 30.5 ± 1.4 mmHg in MA (P = NS). However, there was a significant difference in capillary pressures: 23.6 ± 1.4 mmHg average MC pressure and 28 mmHg calculated mucosal capillary pressure. We suspect that the difference in mucosal and MC pressure profiles was due to a significant postcapillary venous resistance in the mucosa, because a large pressure drop was observed from CV (26.6 ± 1.1 mmHg) through the SMV2 (21.8 ± 1.6 mmHg) and into the SMV1 (17.1 ± 0.8 mmHg). We found that CV, on the mucosal side of muscularis mucosae, were larger in diameter (36.4 ± 1.1 μm) than the following deeper mucosal venous anastomosis (31.5 ± 1.3 μm) or initial part of SMV2, on the submucosal side of muscularis mucosae. Semiquantitative evidence for our argument can be obtained by calculating simple resistance ratios from the pressure and relative flow data.

Assume that gastric muscle and mucosal vasculatures can be represented by two simple parallel circuits with a common input at the level of the SMA1 and a common output at the level of the SMV1. As we described, the drop in arterial pressure down to the MA and MTA was identical. Therefore, intravascular pressures in these arterioles were considered the input values. It is a simple matter to calculate resistance ratios in this model using relative flow data from the microsphere experiments and intravascular pressure data from Fig. 3. Four different resistance ratios were calculated as follows

$$R_{a\,mus}/R_{a\,muc} = (\dot{Q}_{muc}/\dot{Q}_t)(P_{MA} - P_{c\,mus})/(\dot{Q}_{mus}/\dot{Q}_t)/(P_{MTA} - P_{c\,muc}) \quad (1)$$

$$R_{v\,mus}/R_{v\,muc} = (\dot{Q}_{muc}/\dot{Q}_t)(P_{c\,mus} - P_{SMV1})/(\dot{Q}_{mus}/\dot{Q}_t)/(P_{c\,muc} - P_{SMV1}) \quad (2)$$

$$R_{a\,mus}/R_{v\,mus} = (P_{MA} - P_{c\,mus})/(P_{c\,mus} - P_{SMV1}) \quad (3)$$

$$R_{a\,muc}/R_{v\,muc} = (P_{MTA} - P_{c\,muc})/(P_{c\,muc} - P_{SMV1}) \quad (4)$$

where R_a and R_v are the precapillary and postcapillary resistances in the muscle or mucosal vasculature as indicated, $\dot{Q}_{mus}/\dot{Q}_t$ and $\dot{Q}_{muc}/\dot{Q}_t$ represent the fractional blood flow through the muscle and mucosal layer, respectively, and P_{MA}, P_{MTA}, P_{SMV1}, and P_c denote the average pressures in MA, MTA, and SMV1 and corresponding capillaries, respectively. Substituting the appropriate values into *Eqs. 1–4*, we find that

$$R_{a\,mus}/R_{a\,muc} = 0.84\,(30.5 - 23.6)/0.16\,(32.4 - 28) = 8.23 \quad (1a)$$

$$R_{v\,mus}/R_{v\,muc} = 0.84\,(23.6 - 17.1)/0.16\,(28 - 17.1) = 3.13 \quad (2a)$$

$$R_{a\,mus}/R_{v\,mus} = (30.5 - 23.6)/(23.6 - 17.1) = 1.06 \quad (3a)$$

$$R_{a\,muc}/R_{v\,muc} = (32.4 - 28)/(28 - 17.1) = 0.40 \quad (4a)$$

The large values of precapillary ($R_{a\,mus}/R_{a\,muc}$ = 8.23) and postcapillary ($R_{v\,mus}/R_{v\,muc}$ = 3.13) resistance ratios of muscle to mucosal circulations indicate low mucosal vascular resistances. This would be expected, because there are approximately five times as many capillaries in the mucosal circulation as in the muscle vasculature. [If we assume that the microspheres used to measure the relative blood flows were distributed in direct proportion to the number of parallel channels in each tissue region, $(\dot{Q}_{muc}/\dot{Q}_t)/(\dot{Q}_{mus}/\dot{Q}_t)$ = 0.84/0.16 ≈ 5.] In turn, the precapillary-to-postcapillary resistance ratio in the muscle vasculature ($R_{a\,mus}/R_{v\,mus}$ = 1.06) indicates a fairly large equal precapillary and postcapillary resistance in the muscle layer. However, the low mucosal precapillary-to-postcapillary resistance ratio ($R_{a\,muc}/R_{v\,muc}$ = 0.40) suggests that mucosal venules offer high resistance to flow. Therefore, when considered relative to the low mucosal vascular resistances, mucosal venules may be an important determinant of the high mucosal capillary pressure, besides the low precapillary resistance. The relatively high gastric mucosal postcapillary venous resistance is somewhat unique, since very low venular resistances were described in other parts of the intestine (13, 15, 16).

In summary, the present investigation indicates that gastric capillary hydrostatic pressure in the mucosal microcirculation is significantly higher than capillary pressure in the muscle vasculature. Morphological findings and the calculated vascular resistances indicate that the regional difference in capillary pressures may be due to low precapillary, but relatively high postcapillary, resistance in the mucosal microcirculation. Analysis of filtration forces suggests that fluid balance is not maintained in the gastric mucosal microcircula-

tion, which appears to be primarily a filtering network. This conclusion is consistent with the secretory function of this organ.

The authors are grateful to Dr. P. Darwin Bell for critical reading and revision of the manuscript and to S. Adamkó, M. Godó, and G. Nagy for technical assistance.

This work was supported by Hungarian Ministry of Welfare Grant ETT-02290/93, Hungarian Research Foundation Grant OTKA T-017414, and the Semmelweis University Medical School.

Address for reprint requests: L.R. Rosivall, Institute of Pathophysiology, Semmelweis University Medical School, Budapest H-1089, Nagyvárad tér 4, Hungary.

Received 23 March 1998; accepted in final form 25 June 1998.

REFERENCES

1. **Altamirano, M., M. Requena, and T. C. Perez.** Interstitial fluid pressure in canine gastric mucosa. *Am. J. Physiol.* 229: 1414–1420, 1975.
2. **Altamirano, M., M. Requena, and T. C. Perez.** Interstitial fluid pressure and alkaline gastric secretion. *Am. J. Physiol.* 229: 1421–1426, 1975.
3. **Archibald, L. H., F. G. Moody, and M. Simons.** Measurement of gastric blood flow with radioactive microspheres. *J. Appl. Physiol.* 38: 1051–1056, 1975.
4. **Aukland, K., and H. M. Johnsen.** A colloid osmometer for small fluid samples. *Acta Physiol. Scand.* 90: 485–490, 1974.
5. **Benoit, J. N., W. A. Womack, R. J. Korthuis, W. H. Wilborn, and D. N. Granger.** Chronic portal hypertension: effects on gastrointestinal blood flow distribution. *Am. J. Physiol.* 250 (*Gastrointest. Liver Physiol.* 13): G535–G539, 1986.
6. **Bill, A.** Regional lymph flow in unanesthetized rabbits. *Ups. J. Med. Sci.* 84: 129–136, 1979.
7. **Bohlen, H. G., and R. W. Gore.** Preparation of rat intestinal muscle and mucosa for quantitative microcirculatory studies. *Microvasc. Res.* 11: 103–110, 1976.
8. **Boley, S. J., G. P. Agrawal, A. R. Warren, F. J. Veith, B. S. Levowitz, W. Treiber, J. Dougherty, S. S. Schwartz, and M. L. Gleidman.** Pathophysiologic effects of bowel distention on intestinal blood flow. *Am. J. Surg.* 117: 228–234, 1969.
9. **Brobmann, G. F., E. D. Jacobson, and G. A. Brechner.** Intestinal vascular responses to gut pressure and acetylcholine in vitro. *Angiologica* 7: 129–139, 1970.
10. **Chou, C. C., and J. M. Dabney.** Inter-relation of ileal wall compliance and vascular resistance. *Am. J. Dig. Dis.* 12: 1198–1208, 1967.
11. **Chou, C. C., and B. Grassmick.** Motility and blood flow distribution within the wall of the gastrointestinal tract. *Am. J. Physiol.* 235 (*Heart Circ. Physiol.* 4): H34–H39, 1978.
12. **Gannon, B., J. Browning, and P. O'Brien.** The microvascular architecture of the glandular mucosa of rat stomach. *J. Anat.* 135: 667–683, 1982.
13. **Gore, R. W., and H. G. Bohlen.** Microvascular pressures in rat intestinal muscle and mucosal villi. *Am. J. Physiol.* 233 (*Heart Circ. Physiol.* 2): H685–H693, 1977.
14. **Gore, R. W., and H. G. Bohlen.** Pressure regulation in the microcirculation. *Federation Proc.* 34: 2031–2037, 1975.
15. **Granger, D. N., and J. A. Barrowman.** Microcirculation of the alimentary tract. I. Physiology of transcapillary fluid and solute exchange. *Gastroenterology* 84: 846–868, 1983.
16. **Granger, D. N., M. A. Perry, and P. R. Kvietys.** The microcirculation and fluid transport in digestive organs. *Federation Proc.* 42: 1667–1672, 1983.
17. **Guth, P. H., and A. Rosenberg.** In vivo microscopy of the gastric microcirculation. *Am. J. Dig. Dis.* 17: 391–398, 1972.
18. **Hanson, K. M., and F. T. Moore.** Pressure-volume relationships and blood flow in the distended colon. *Am. J. Physiol.* 217: 35–39, 1969.
19. **Holm, L.** Gastric mucosal blood flow and mucosal protection. *J. Clin. Gastroenterol.* 10, *Suppl.* 1: S114–S119, 1988.
20. **Intaglietta, M., R. F. Pawula, and W. R. Tompkins.** Pressure measurements in the mammalian microvasculature. *Microvasc. Res.* 2: 212–220, 1970.
21. **Intaglietta, M., and W. R. Tompkins.** Micropressure measurement with 1 μm and smaller cannulae. *Microvasc. Res.* 3: 211–214, 1971.
22. **Jackson, W. F., and B. R. Duling.** The oxygen sensitivity of hamster cheek pouch arterioles. In vitro and in situ studies. *Circ. Res.* 53: 515–525, 1983.
23. **Jacobson, E. D., G. F. Brobmann, and G. A. Brechner.** Intestinal motor activity and blood flow. *Gastroenterology* 58: 575–579, 1970.
24. **Kowallik, P., R. Schulz, B. Guth, A. Schade, W. Paffhausen, R. Gross, and G. Heusch.** Measurement of regional myocardial blood flow with multiple colored microspheres. *Circ. Res.* 83: 974–982, 1991.
25. **Lombard, J. H., and W. J. Stekiel.** Effect of oxygen on arteriolar diameters in the rat mesoappendix. *Microvasc. Res.* 30: 346–349, 1985.
26. **Mortillaro, N. A., and A. E. Taylor.** Interaction of capillary and tissue forces in the cat intestine. *Circ. Res.* 39: 348–358, 1976.
27. **Ohno, T., M. Katori, K. Nishiyama, and K. Saigenji.** Direct observation of microcirculation of the basal region of rat gastric mucosa. *J. Gastroenterol.* 30: 557–564, 1995.
28. **Perry, M. A., W. J. Crook, and D. N. Granger.** Permeability of gastric capillaries to small and large molecules. *Am. J. Physiol.* 241 (*Gastrointest. Liver Physiol.* 4): G478–G486, 1981.
29. **Peti-Peterdi, J., P. Hamar, G. Kovacs, and L. Rosivall.** Direct in-vivo measurement of gastric microvascular pressures in the rat. *Microvasc. Res.* 55: 223–229, 1998.
30. **Phillips, R. A., D. D. Van Slyke, P. B. Hamilton, V. P. Dole, K. Emerson, Jr., and R. M. Archibald.** Measurement of specific gravities of whole blood and plasma by standard copper sulfate solutions. *J. Biol. Chem.* 183: 305–330, 1950.
31. **Ritchie, W. P., Jr.** Acute gastric mucosal damage induced by bile salts, acid and ischemia. *Gastroenterology* 68: 699–707, 1975.
32. **Rosenberg, A., and P. H. Guth.** A method for the in vivo study of the gastric microcirculation. *Microvasc. Res.* 2: 111–112, 1970.
33. **Sidky, M., and J. W. Bean.** Influence of rhythmic and tonic contraction of intestinal muscle on blood flow and blood reservoir capacity in dog intestine. *Am. J. Physiol.* 193: 386–392, 1958.
34. **Sullivan, S. M., and P. C. Johnson.** Effect of oxygen on arteriolar dimensions and blood flow in cat sartorius muscle. *Am. J. Physiol.* 241 (*Heart Circ. Physiol.* 10): H547–H556, 1981.
35. **Wiedeman, M. P.** Blood flow through terminal arterial vessels after denervation of the bat wing. *Circ. Res.* 22: 83–89, 1968.
36. **Wiederhielm, C. A., J. W. Woodbury, S. Kirk, and R. F. Rushmer.** Pulsatile pressures in the microcirculation of frog's mesentery. *Am. J. Physiol.* 207: 173–176, 1964.
37. **Yabana, T., and A. Yachi.** Seminars on gastric mucosal injury. VI. Stress-induced vascular damage and ulcer. *Dig. Dis. Sci.* 33: 751–761, 1988.
38. **Zweifach, B. W., and M. Intaglietta.** Measurement of blood plasma colloid osmotic pressure. II. Comparative study of different species. *Microvasc. Res.* 3: 83–88, 1971.